Magyarhoni Földtani Társulat
Földtani Közlöny
Hungarian Geological Society

153/2, 129–142., Budapest, 2023

DOI: 10.23928/foldt.kozl.2023.153.2.129

Mineralogical mosaics from the Carpathian-Pannonian region 5

ZAJZON, Norbert[1], SZAKÁLL, Sándor[1], FEHÉR, Béla[2], KRISTÁLY, Ferenc[1]

[1]Institute of Exploration Geosciences, University of Miskolc, H-3515 Miskolc-Egyetemváros, Hungary
[2]Department of Mineralogy, Herman Ottó Museum, Kossuth u. 13, H-3525 Miskolc, Hungary

Ásványtani mozaikok a Kárpát–Pannon régióból 5.

Összefoglalás

Ötödik tanulmányunkban további mozaikszerű adatokkal dokumentáljuk a Kárpát–Pannon régió ásványvilágát. Az új adatokat országok és lelőhelyek szerint csoportosítottuk. Az egyes „mozaikdarabokban" az ásványok pontos leírására és – döntően XRPD, SEM-EDX és EMPA általi – meghatározására, illetve a paragenezis tömör bemutatására koncentráltunk. A tanulmányunkban szereplő ásványok olykor első említések az egész régióból vagy legalábbis az illető lelőhelyről.

Magyarországról a bicske-csordakúti széntelepből humboldtin és weddellit, a recski Lahóca ércesedéséből Sr-gazdag és más APS- (alumínium-foszfát-szulfát-) ásványok vizsgálati adatait közöljük.

Romániából a Hargita vulkáni vonulatából Mg-gazdag turmalinok kémiai adatait közöljük, míg a felsőbányai (Baia Sprie) ércesedésből kirgizisztánit jelenlétét dokumentáljuk.

Szlovákiából a farbištei (Pónik/Poniky) ércesedésből Na-tartamú szulfátok (kröhnkit, ferrinátrit, tamarugit), a rozsnyói (Rožňava) ércesedésből egy arzenát, a bariofarmakosziderit kimutatását ismertetjük.

Kulcsszavak: bariofarmakosziderit, crandallit, drávit, ferrinátrit, foitit, goyazit, hinsdalit, humboldtin, kirgizisztánit, kröhnkit, magneziofoitit, svanbergit, turmalin, weddellit, woodhouseit

Abstract

Further mosaic-like data were recorded on the mineral occurrences of the Carpathian–Pannonian region in this fifth member of the series arranged by countries and localities. Each "mosaic" contains a concise mineral description, mainly based on XRPD, SEM-EDX and EPMA measurements and a concise description of the mineral paragenesis. Some minerals are first-time descriptions from the entire discussed region, but all are newly documented occurrences for at least the described locality.

From Hungary humboldtine and weddellite are described from the coalbed of Csordakút (Bicske), and data from Sr-rich and other Aluminium Phosphate Sulphate (APS) minerals from the ore mineralization of the Lahóca Hill at Recsk are also reported.

Chemical data of Mg-rich tourmaline from the Harghita volcanic ridge are given, and also kyrgyzstanite is described from the ore mineralization of Baia Sprie, Romania.

From Slovakia Na-containing sulphates (kröhnkite, ferrinatrite, tamarugite) from the ore mineralization of Farbište (Poniky) and an arsenate (bariopharmacosiderite) from the ore mineralization of Rožňava are also introduced.

Keywords: bariopharmacosiderite, crandallite, dravite, ferrinatrite, foitite, goyazite, hinsdalite, humboldtine, kröhnkite, kyrgyzstanite, magnesio-foitite, svanbergite, tourmaline, weddellite, woodhouseite

The minerals described in the paper

Here we present the minerals we describe in the paper as a table (*Table 1)* to help the reading of the article with their ideal composition, the locality where the mineral was found and also the method, which was used for the identification.

Experimental methods and samples

X-ray powder diffraction (XRPD) patterns of ferrinatrite, tamarugite, kröhnkite, weddellite and humboldtine were recorded on a Bruker D8 Advance diffractometer using CuK_a radiation (40 kV and 40 mA) with a 250 mm-

Table I. List of identified minerals with their theoretical formulae, locality and identification method
I. táblázat. *Az azonosított ásványok ideális képletükkel, lelőhelyükkel és az azonosítás módjával*

Mineral names	Ideal formula	Locality	Identification method
Bariopharmacosiderite	$Ba_{0.5}Fe^{3+}_4(AsO_4)_3(OH)_4 \cdot 5H_2O$	Štefan gallery of Nadabula, Rožňava ore deposit, Sk	SEM-EDX
Crandallite	$CaAl_3(PO_4)(PO_3OH)(OH)_6$	Lahóca Hill, Recsk, Hu	WDX
Dravite	$NaMg_3Al_6(Si_6O_{18})(BO_3)_3(OH)_3(OH)$	Mădăraş (Şarogag) and Sântimbru Băi, Harghita Mts., Ro	WDX
Ferrinatrite	$Na_3Fe^{3+}(SO_4)_3 \cdot 3H_2O$	Farbište ore deposit, Poniky, Sk	XRPD, SEM-EDX
Foitite	$\square(Fe^{2+}_2Al)Al_6(Si_6O_{18})(BO_3)_3(OH)_3(OH)$	Mădăraş (Şarogag) and Sântimbru Băi, Harghita Mts., Ro	WDX
Goyazite	$SrAl_3(PO_4)(PO_3OH)(OH)_6$	Lahóca Hill, Recsk, Hu	WDX
Hinsdalite	$PbAl_3(SO_4)(PO_4)(OH)_6$	Lahóca Hill, Recsk, Hu	WDX
Humboldtine	$Fe^{2+}(C_2O_4) \cdot 2H_2O$	Csordakút coal mine, Bicske, Hu	XRPD, SEM-EDX, FTIR
Kröhnkite	$Na_2Cu(SO_4)_2 \cdot 2H_2O$	Farbište ore deposit, Poniky, Sk	XRPD, SEM-EDX
Kyrgyzstanite	$ZnAl_4(SO_4)(OH)_{12} \cdot 3H_2O$	Dealul Minei, Baia Sprie, Ro	XRPD, SEM-EDX
Magnesio-foitite	$\square(Mg_2Al)Al_6(Si_6O_{18})(BO_3)_3(OH)_3(OH)$	Mădăraş (Şarogag) and Sântimbru Băi, Harghita Mts., Ro	WDX
Svanbergite	$SrAl_3(SO_4)(PO_4)(OH)_6$	Lahóca Hill, Recsk, Hu	WDX
Weddellite	$Ca(C_2O_4) \cdot 2H_2O$	Csordakút coal mine, Bicske, Hu	XRPD, SEM-EDX
Woodhouseite	$CaAl_3(SO_4)(PO_4)(OH)_6$	Lahóca Hill, Recsk, Hu	WDX

radius goniometer, in parallel-beam geometry obtained by Goebel-mirror optics, 0.25° primary axial Soller with a 0.6-mm divergence slit and position sensitive Vantec-1 detector (1° opening). Samples of 1 to 5 mg were ground in agate mortar under acetone and loaded on low-background (Si crystal) sample holders. All patterns were recorded in the 2–70° (2Θ) range with 0.007° (2Θ) / 4 sec scanning rate.

X-ray diffraction study was also performed with a 114.6 mm diameter Gandolfi camera for kyrgyzstanite. Analytical parameters: CuK_a radiation, Ni filter, 40 kV accelerating voltage, 25 mA tube current, exposition time 47 hours.

Scanning electron microscopy (SEM) studies, energy-dispersive X-ray spectroscopy (EDX), X-ray mapping and electron microprobe measurements (EMPA) were done on a JEOL JXA-8600 Superprobe unit equipped with four wavelength-dispersive spectrometers and an EDX silicon drift detector (SDD) at the Institute of Exploration Geosciences, University of Miskolc. For the EDX measurements 15–20 kV accelerating voltage was used, with a probe current of 10–20 nA. A 4 × 5 μm area was scanned with focused beam during the analyses (stopped focused beam was used if the target area was too small).

Quantitative electron microprobe analyses were performed at the Geological Institute of Dionýz Štúr, Bratislava, Slovakia. For the analyses of svanbergite, goyazite, hinsdalite, woodhouseite, crandallite and tourmaline, a Cameca SX-100 instrument was used in wavelength-dispersive mode. Operating conditions were as follows: accelerating voltage 15 kV, probe current 20 nA. Analytical standards: apatite (P), GaAs (As), orthoclase (Si, K), TiO_2 (Ti), Al_2O_3 (Al), fayalite (Fe), forsterite (Mg), wollastonite (Ca), rhodonite (Mn), willemite (Zn), $SrTiO_3$ (Sr), baryte (S, Ba), $PbCO_3$ (Pb), albite (Na) and LiF (F). Raw intensity data were corrected using a PAP matrix correction.

Almost all the investigated samples are part of the mineral collection of the Herman Ottó Museum, Miskolc, Hungary (inventory numbers: 2022.37 for weddellite, Bicske; 2021.127 for APS minerals, Recsk; 2021.129 for tourmaline, Harghita; 2022.111 for kröhnkite and ferrinatrite, Poniky), except for a few bariopharmacosiderite samples from the Hungarian Natural History Museum (MTM - Á.60.5256.), a few humboldtine samples from Supervisory Authority of Regulatory Affairs (MÁFI - AT.2008.1206.1.), and, finally, the kyrgyzstanite sample, which is from Gábor Koller's private collection.

Results

Hungary

Humboldtine and weddellite from Csordakút coal mine, Bicske

The Eocene coal bed of Csordakút, Bicske is famous for its giant (up to 10 cm) mellite crystals found in the late 1970s (Weiszburg et al. 2000). Close to this location, a gypsum–whewellite mineral association was published by Papp (1990) from the so-called "mellite-bearing layer" just underlying the coal bed. Whewellite was found as 0.1–0.2 mm, elongated, columnar crystals together with gypsum crystals of similar size in loose clusters up to a few dm in size. Associated with mellite, up to few-mm-long lath-like crystals were found as parallel grown, fibrous veinlet-forming masses. Rare weddellite was found by XRPD (*Figure 1*) and SEM-EDX with more abundant gypsum and whewellite. The two hydrous oxalates can be distinguished from each other based on morphology. The 1.5 mm long, lath-like crystals of weddellite forms fibrous masses, whereas the

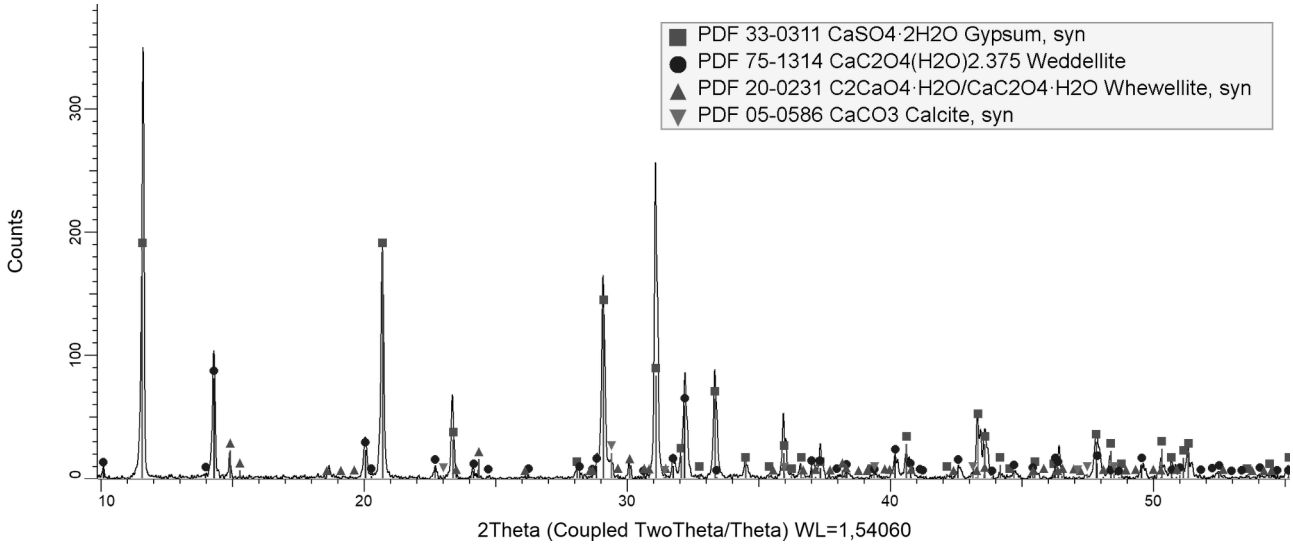

Figure 1. X-ray powder diffraction pattern of a weddellite-containing sample from the Csordakút coal mine, Bicske, Hungary
1. ábra. *Egy bicske-csordakúti weddellittartalmú minta röntgenpordiffrakciós felvétele*

crystals of whewellite are tabular with 0.1–0.2 mm size (*Figure 2*). A part of whewellite was most likely formed from weddellite by dehydration. Weddellite and whewellite association in cherty concretions from lake-bottom sediments was first described by MANDARINO & WILL (1983), who explained the formation of whewellite in part by the dehydration of weddellite. It could be a similar situation in Csordakút, where we assume that the primary Ca oxalate was the more hydrous weddellite. Both oxalates were formed from calcium- and oxalic acid-containing fluids. The latter fluid was produced during the decay of organic materials.

We also identified the following minerals in the mellite-containing layer: fine, hair-like halotrichite, pyrite as disseminated minute framboids, allophane as glassy encrustations, earthy gibbsite, pale yellow, earthy ammoniojarosite and jarosite, and, finally, alunite concretions, 1–3 mm in diameter. The sulphates possibly formed by pyrite oxidation. Two V-containing – yet unidentified – phases (possibly V-Al oxides) should also be mentioned. These are closely associated with kaolinite and gypsum. Humboldtine shows more intense yellow colour than ammoniojarosite and forms porous, earthy masses, which rarely reach 10–15 cm. These masses can also be found in the cracks of the enclosing claystone. In some places, this type of humboldtine is penetrated by mellite veinlets, and less typically occurs as inclusions in mellite crystals. In the latter case, mellite contains yellow patches. The most spectacular humboldtine variety forms 0.5–1.5 cm irregular aggregates on mellite crystals. These aggregates are built up by 10–30 μm sized tabular crystals (*Figure 3*). Humboldtine also forms lenticular, honey-yellow crystals enclosed in masses of gypsum and an undetermined V-Al-oxide (*Figure 4*). These crystals can reach

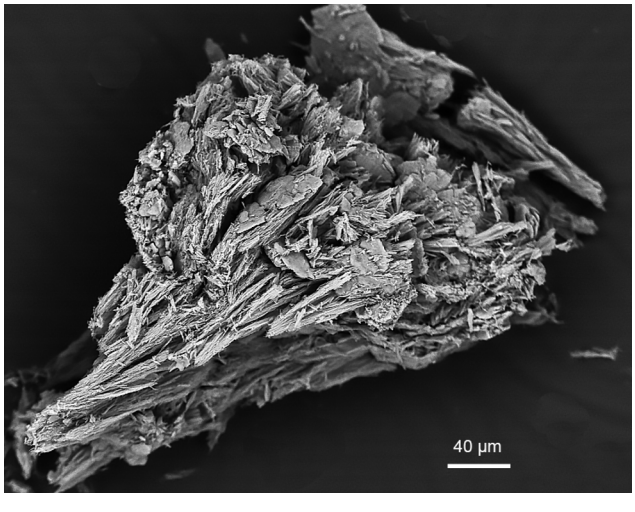

Figure 2. Lath-like weddellite with tabular whewellite from the Csordakút coal mine, Bicske, Hungary. BSE image. Photo courtesy of Á. KOVÁCS
2. ábra. *Léces weddellit és táblás whewellit együttese. Csordakúti szénbánya (Bicske). Visszaszórtelektron-kép. Fotó: KOVÁCS Á.*

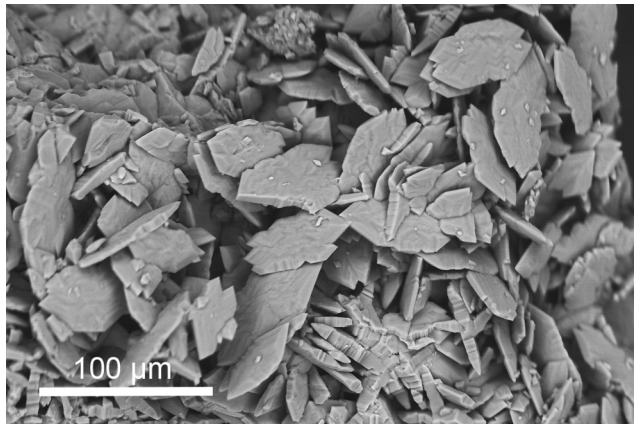

Figure 3. Tabular crystals of humboldtine from the Csordakút coal mine, Bicske, Hungary. BSE image. Photo courtesy of Á. KOVÁCS
3. ábra. *Humboldtin táblás kristályai. Csordakúti szénbánya (Bicske). Visszaszórtelektron-kép. Fotó: KOVÁCS Á.*

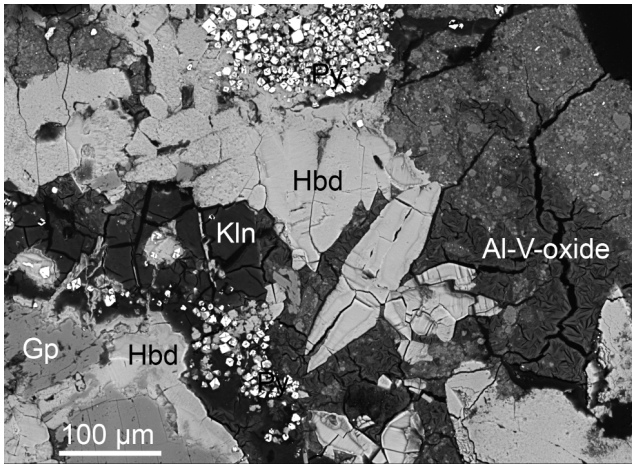

Figure 4. Lenticular humboldtine crystals (Hbd) in a V-Al oxide (dark grey) and gypsum (Gp, light grey) with pyrite (white) and kaolinite (Kln, black) from the Csordakút mine, Bicske. BSE image

4. ábra. *Lencse alakú humboldtinkristályok (Hbd) V-Al-oxid-ásványban (sötétszürke) és gipszben (Gp, világosszürke), pirittel (fehér) és kaolinittel (Kln, fekete). Csordakúti szénbánya (Bicske). Visszaszórtelektron-kép*

100–200 µm size. The above-described minerals were identified by XRPD, FTIR and SEM-EDX. The measured XRPD data can be found in *Table II*, and the FTIR spectrum is shown in *Figure 5*. The authigenic formation of humboldtine together with other organic minerals in coal seams is well-known, although its paragenetic association with the large mellite crystals is a worldwide rarity.

Sr- and Ca-rich APS minerals from Lahóca epithermal ore deposit, Recsk

Strontium-, calcium- and lead-rich aluminium phosphate sulphate (APS) minerals with broadly varying chemical substitutions were identified by WDX from the high-sulphidation (HS) deposit of Lahóca Hill. The crystals are white rhombohedra, 0.1–0.2 mm in size, and their external zones dominantly have crandallite composition. They always appear in the voids of siliceous vein fillings. The first samples were found in the waste dump of the Ferenc gallery, later they were also described from other dumps from the southern side of Lahóca Hill. A genetical study of the Lahóca Hill ore mineralization by Molnár et al. (2008) also describe the zonation of the epithermal rock alterations, but do not mention any APS minerals at all. Szakáll et al. (1994) mention crandallite from the area firstly from the nearby Parádfürdő ore mineralization. The APS mineral formation in general is divided into four stages according to Dill (2001), where the first stage – hypogene phosphate-sulphate formation – is characterized by the Ca-rich APS minerals (like woodhouseite, crandallite). In Recsk we can find exactly these phases with the addition of Sr-rich species; from the crandallite group: crandallite and goyazite and from the woodhouseite group: woodhouseite, svanbergite and hinsdalite. One typical attribute of the hydrothermal APS minerals is the chemical heterogeneity, caused by the significant changes in the physical-chemical parameters during crystallization. In addition, APS minerals can incorporate a large variety of elements into their structure, which may lead to the formation of zones with different compositions. In Recsk, we observed the following APS mineral types and characteristics: the core of the crystals is usually Sr-rich, thus they are Ca-rich svanbergite, Ca-S-rich goyazite, Sr-rich woodhouseite, and rarely Sr-rich crandallite (*Appendix I.*, *Figure 6*). The Sr-rich inner part is followed by Pb-rich zones, as Ca-rich hinsdalite or Pb-rich woodhouseite, whereas the outermost zones are formed by S-rich or S-Pb-rich crandallite (*Figures 7* and *8*). According to the analyses, the substitutions in the divalent *A* position from the core to rim

Table II. X-ray powder diffraction data of humboldtine from the Csordakút mine, Bicske, compared with those of the ICDD 00-023-0293 card

II. táblázat. *A csordakúti (Bicske) humboldtin röntgenpordiffrakciós adatai, összehasonlítva az ICDD 00-023-0293 kártya adataival*

Humboldtine Bicske		Humboldtine ICDD 00-023-0293				
d (Å)	*I* (%)	*d* (Å)	*I* (%)	*h*	*k*	*l*
4.801	100	4.800	100	2	0	0
4.700	65	4.700	65	0	0	2
3.878	24	3.880	25	−2	0	2
3.624	20	3.629	20	−2	1	1
3.591	23	3.597	25	−1	1	2
3.167	3	3.172	4	1	1	2
3.004	42	3.004	50	2	0	2
2.773	3	2.778	4	0	2	0
2.652	26	2.654	30	−3	1	2
2.630	15	2.634	16	−2	1	3
2.611	21	2.616	25	−1	2	1
2.394	2	2.396	3	−4	0	2
2.356	2	2.355	3	−2	0	4
2.256	10	2.258	13	−2	2	2
2.223	3	2.224	3	−1	1	4
2.190	3	2.190	4	3	1	2
2.121	7	2.122	9	−3	2	1
2.103	6	2.106	8	−1	2	3
2.035	6	2.037	7	−4	1	3
2.021	11	2.021	14	−3	1	4
1.978	2	1.980	3	3	2	1
1.950	8	1.949	11	4	0	2
1.929	7	1.929	9	2	0	4
1.891	12	1.893	15	−3	2	3
1.846	2	1.847	2	−5	1	2
1.815	16	1.816	21	−2	1	5
1.793	3	1.795	4	0	2	4
1.780	2	1.779	2	0	1	5
1.725	2	1.727	3	−2	3	1
1.671	2	1.673	2	2	3	1
1.635	3	1.635	4	4	1	3
1.624	2	1.625	3	3	2	3
1.613	1	1.613	2	−2	0	6
1.589	4	1.590	5	−4	2	4
1.548	2	1.547	3	−1	1	6
1.507	4	1.508	5	5	2	1
1.488	2	1.489	3	1	2	5
1.457	2	1.458	3	2	3	3
1.371	3	1.372	3	−7	1	2
1.365	4	1.367	5	−1	4	1
1.351	2	1.353	2	1	4	1

Unit cell refined: *I*2/*a* space group, a = 9.917 Å, b = 5.546 Å, c = 9.707 Å, β = 104.46°, V = 517.069 Å^3.

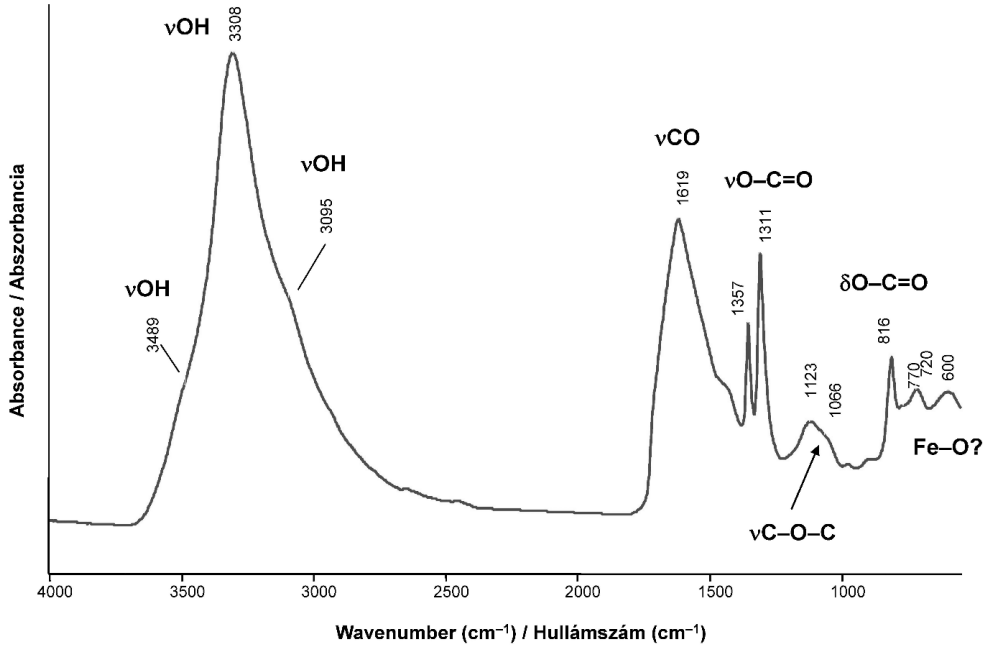

Figure 5. FTIR spectrum of humboldtine from the Csordakút mine, Bicske, Hungary (analyst: J. MIHÁLY)
5. ábra. *A csordakúti (Bicske) humboldtin FTIR-spektruma (MIHÁLY J. felvétele)*

are as follows: Sr(Ca) → Pb → Ca. The trivalent *B* site is always Al-dominant. The Pb-rich zones around the core represent the second stage of DILL's (2001) system. Contrary to the model of DILL, in the third stage (transition from hypogene to supergene formation) the APS-minerals become enriched in phosphate simultaneously with sulphate depletion. According to DILL (2001), typically in crandallite-group minerals the most common cations in the *A* position are Ba and REE. In Recsk, crandallite is the typical APS mineral in the rims, occasionally with Ba-enrichment (see *Figures 7* and *8*). In one case, a REE-dominant phase, florencite-(Ce), was found as a few μm-thin crust on a crystal, but it could not be analysed quantitatively due to its minuscule size.

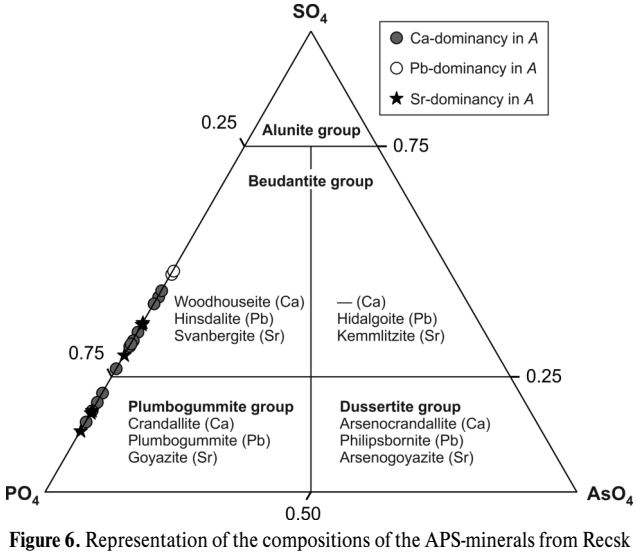

Figure 6. Representation of the compositions of the APS-minerals from Recsk in the PO_4-AsO_4-SO_4 ternary diagram, where B = Al, indicating the names of Ca-, Pb- and Sr-dominant species (in the A-site) according to the current nomenclature (BAYLISS et al. 2010). The boundaries of each compositional field were plotted based on SCOTT (1987).
6. ábra. *A recski APS-ásványok összetételének ábrázolása a PO_4-AsO_4-SO_4 háromszögdiagramban, ahol B = Al, feltüntetve az A-pozícióban Ca-, Pb- és Sr-domináns fajok neveit a jelenlegi nevezéktan szerint (BAYLISS et al. 2010). Az egyes összetételi mezők határait SCOTT (1987) alapján ábrázoltuk.*

Romania

Magnesium-rich tourmalines (magnesio-foitite, foitite, dravite) from hydrothermal mineralizations in the Harghita Mountains

Tourmalinization – a less common rock alteration process – is a well-known phenomenon in the Călimani-Gurghiu-Harghita volcanic range of the East Carpathians. The first reference to tourmaline was made by STANCIU (1976) from the caldera of Ostoroş, where tourmaline was observed

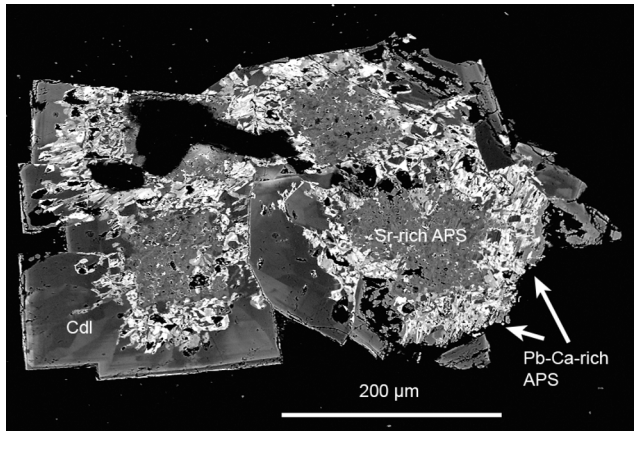

Figure 7. Chemical zoning of APS minerals from Ferenc gallery, Lahóca ore deposit, Recsk, Hungary. BSE image. Photo courtesy of V. KOLLÁROVÁ
7. ábra. *Kémiailag zónás APS-ásványok. Recsk, lahócai ércesedés, Ferenc-táró. Visszaszórtelektron-kép. Fotó: V. KOLLÁROVÁ*

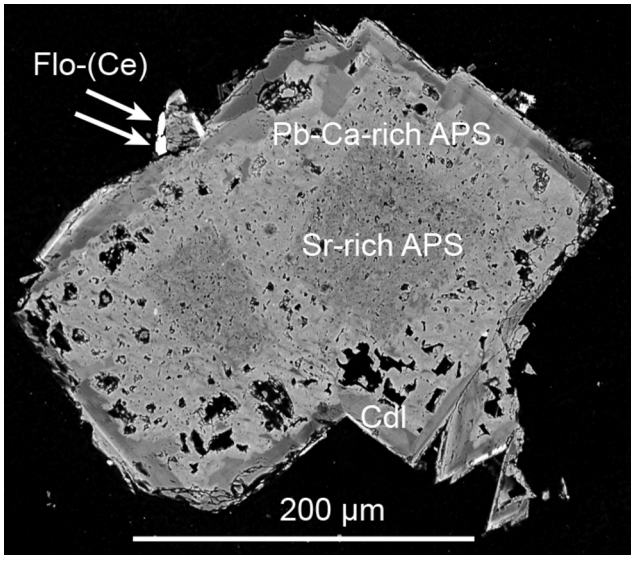

Figure 8. Chemical zoning of APS minerals from Ferenc gallery, Lahóca ore deposit, Recsk, Hungary. BSE image. Photo courtesy of V. KOLLÁROVÁ

8. ábra. *Kémiailag zónás APS-ásványok. Recsk, lahócai ércesedés, Ferenc-táró. Visszaszórtelektron-kép. Fotó: V. KOLLÁROVÁ*

as cement material in a hydrothermally silicified volcanic rocks. Later it was recognized from numerous localities (see SZAKÁLL & KRISTÁLY 2010) and described as dravite or simply tourmaline. The chemical analyses of colourless or pale blue tourmalines of silicified volcanic rocks from two localities Mădăraş (Şarogag) and Sântimbru Băi (Hg-ore occurrence) are tabulated in *Appendix II*. Although the Ca content is high (0.12–0.34 *apfu*), the *X*-site is dominated by either vacancies or, in two analyses (columns 3 and 5), sodium. Where the number of vacancies in the *X*-position exceeds that of both sodium and calcium, the compositions correspond to either magnesio-foitite ($Mg^Y > Fe^Y$) or foitite ($Fe^Y > Mg^Y$), depending on the Fe and Mg content in the *Y*-site. In the two analytical points where Na is the dominant *X*-cation, the chemistry of tourmaline corresponds to dravite, since $Mg^Y > Fe^Y$ (see HENRY et al. 2011 for the nomenclature of tourmaline-supergroup minerals). No chemical zonation was observed in the crystals. The length of the individual crystals is 0.2–0.5 mm, they build radial-spherical aggregates up to 1–1.5 mm in size (*Figures 9* and *10*). Tourmalines with similar composition were published from similar epithermal rocks of the Carpathians, from the Börzsöny and from the Vihorlat Mts. (FEHÉR et al. 2016, FEHÉR 2017). Quartz and kaolinite are associated with tourmalines in the investigated localities.

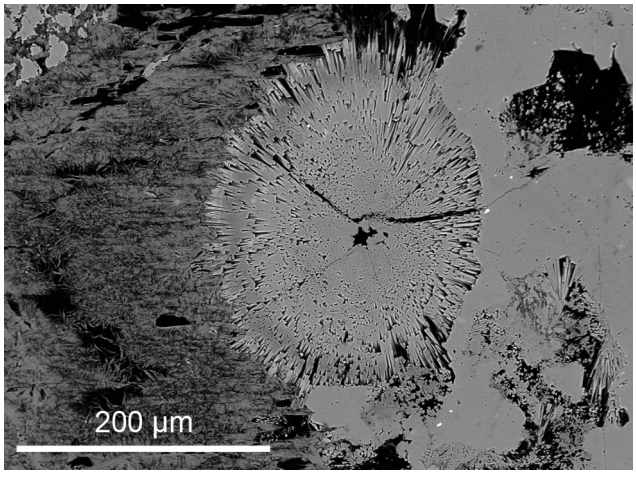

Figure 9. Radial aggregate of tourmaline crystals in quartz and kaolinite matrix. Mercury-ore occurrence, Sântimbru Băi, Romania. BSE image. Photo courtesy of V. KOLLÁROVÁ

9. ábra. *Turmalinkristályok sugaras halmaza kvarcban és kaolinitben. Csíkszentimrei Büdösfürdő, higanyérc-indikáció (Románia). Visszaszórtelektron-kép. Fotó: V. KOLLÁROVÁ*

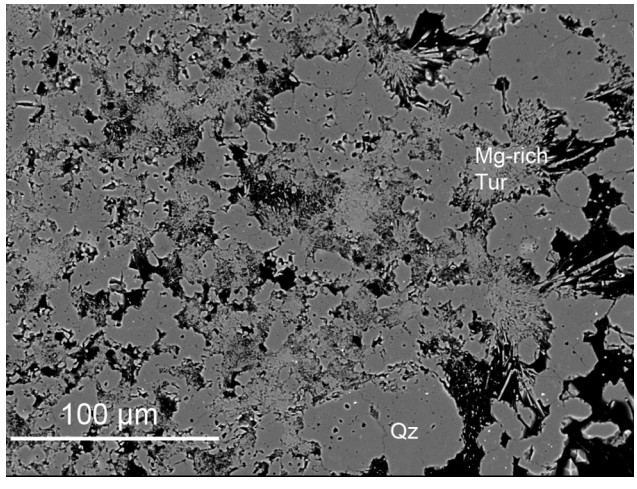

Figure 10. Radial aggregate of tourmaline crystals in quartz matrix. Şarogag, Mădăraş, Romania. BSE image. Photo courtesy of V. KOLLÁROVÁ

10. ábra. *Turmalinkristályok sugaras halmaza kvarcban. Csíkmadaras, Sárogág (Románia). Visszaszórtelektron-kép. Fotó: V. KOLLÁROVÁ*

Kyrgyzstanite from Baia Sprie (Felsőbánya) ore deposit

In a historical specimen from Dealul Minei, Baia Sprie (more precise location is unknown) masses of stibnite needles in quartz veinlets were observed. White spheres of kyrgyzstanite, 0.1–0.2 mm sized, were found overgrown on

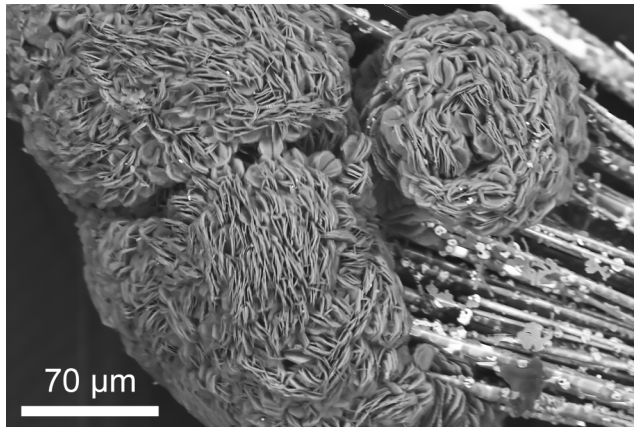

Figure 11. Globular aggregates of kyrgyzstanite on stibnite. Dealu Minei ore deposit, Baia Sprie, Romania. BSE image

11. ábra. *Kirgizisztánit gömbös halmazai antimoniton. Felsőbánya, Bánya-hegyi ércesedés (Románia). Visszaszórtelektron-kép*

stibnite and together with rare Mn-rich siderite rhombohedrons. The spherical masses of kyrgyzstanite are built up by scaly crystals (*Figure 11*). The scattered scales of kyrgyzstanite were also observed as loose encrustations on the stibnite needles. The mineral was identified based on XRPD (*Table III*) and SEM-EDX analyses (it contains Zn, Al and S elements). Zn might have been supplied by supergene oxidation of sphalerite, whereas the different clay minerals were the source of aluminium.

Table III. X-ray powder diffraction data of kyrgyzstanite from Baia Sprie in comparison with those of the type material (AGAKHANOV et al. 2005)

III. táblázat. *A felsőbányai kirgizisztánit röntgen-pordiffrakciós adatai, összehasonlítva a típusásvány megfelelő adataival (AGAKHANOV et al. 2005)*

Kyrgyzstanite Baia Sprie		Kyrgyzstanite (AGAKHANOV et al. 2005)				
d (Å)	*I* (%)	*d* (Å)	*I* (%)	*h*	*k*	*l*
8.56	100	8.60	100	0	0	2
7.89	22	7.93	70	0	1	1
4.80	6	4.83	80	0	1	3
4.60	12	4.61	20	2	0	–2
4.26	49	4.27	100	0	0	4
3.565	5	3.50	20	0	2	3
3.353	3	3.35	30	1	0	–5
3.189	6	3.19	50	0	1	5
3.057	17	3.05	50	3	1	1
2.768	5	2.79	10	2	2	3
2.726	5	2.72	50	1	3	–2
2.522	19	2.51	70	4	0	–2
2.298	21	2.29	80	4	1	2
2.225	6	2.23	30	4	1	–4
2.105	3	2.09	20	4	1	–5
2.004	20	1.99	95	2	4	–2
1.918	2	1.89	65	3	2	–7
1.816	3	1.80	40	2	4	4
1.727	8	1.72	65	2	3	7
1.693	2	1.69	20	3	3	6
1.563	3	1.55	50	1	3	9
1.486	8	1.48	40	2	2	10
1.463	7	1.46	30	2	5	–6
1.404	3	1.39	30	7	0	–5
1.358	2	1.35	40	3	5	–7

Slovakia

Kröhnkite and ferrinatrite from Farbište ore deposit, Poniky (Pónik)

Numerous secondary minerals (arsenates, oxides, carbonates) were identified earlier (see KODĚRA 1986) from the alteration of the primary Cu sulphides of the copper mineralization of Farbište (Poniky, Banská Bystrica district). Here we describe some rare sulphates, which are new for the locality. Among them, the most interesting ones are the Na-containing phases. The recently formed sulphates can be found as porous aggregates, sprays in the cracks of a strongly altered, argillised and silicified rock. Associated with common gypsum, chalcanthite and jarosite, the described

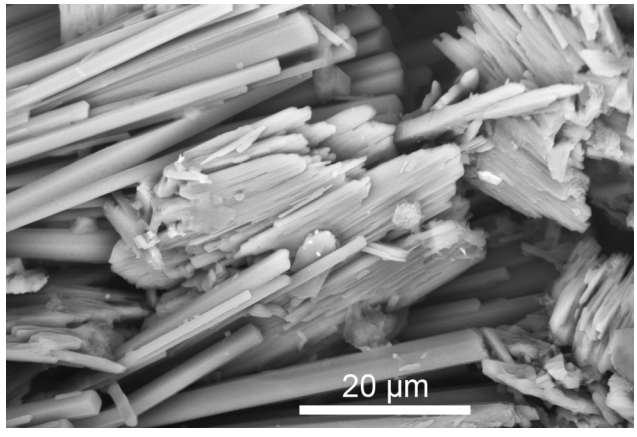

Figure 12. Prismatic kröhnkite crystals. Farbište ore deposit, Poniky, Slovakia. SEM image

12. ábra. *Oszlopos kröhnkitkristályok. Pónik, Farbište érctelep (Szlovákia). Pásztázó elektronmikroszkópos felvétel*

Na-containing phases are kröhnkite, tamarugite and ferrinatrite. Kröhnkite is pale blue, it forms 0.1 mm long needles or columnar crystals (*Figure 12*). Ferrinatrite forms white, elongated prisms or scaly masses with pearly lustre in close association with kröhnkite (*Figure 13*). Tamarugite forms acicular masses, whereas the associated chalcanthite occurs as light blue crusts and jarosite appears as yellow, irregular aggregates. They were identified by XRPD and SEM-EDX analyses. A diffractogram of a mixture of ferrinatrite-kröhnkite-tamarugite is shown in *Figure 14*, while *Appendix III* contains the XRPD data of kröhnkite.

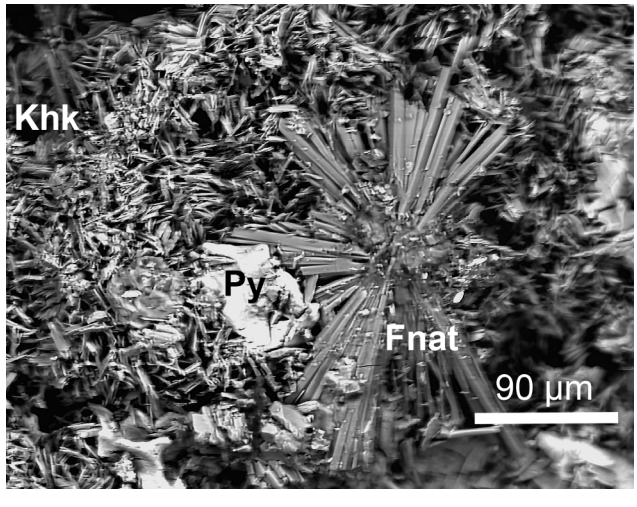

Figure 13. Prismatic ferrinatrite crystals (Fnat), associated with kröhnkite (Khk). Farbište ore deposit, Poniky, Slovakia. BSE image

13. ábra. *Oszlopos ferrinátritkristályok (Fnat) kröhnkit (Khk) társaságában. Pónik, Farbište érctelep (Szlovákia). Visszaszórtelektron-kép*

Bariopharmacosiderite from Rožňava (Rozsnyó) ore deposit

Scorodite formed by the alteration of tetrahedrite in the Rožňava ore deposit – more precisely in the Štefan (István) gallery of Nadabula (Sajóháza) – was first mentioned by ZI-

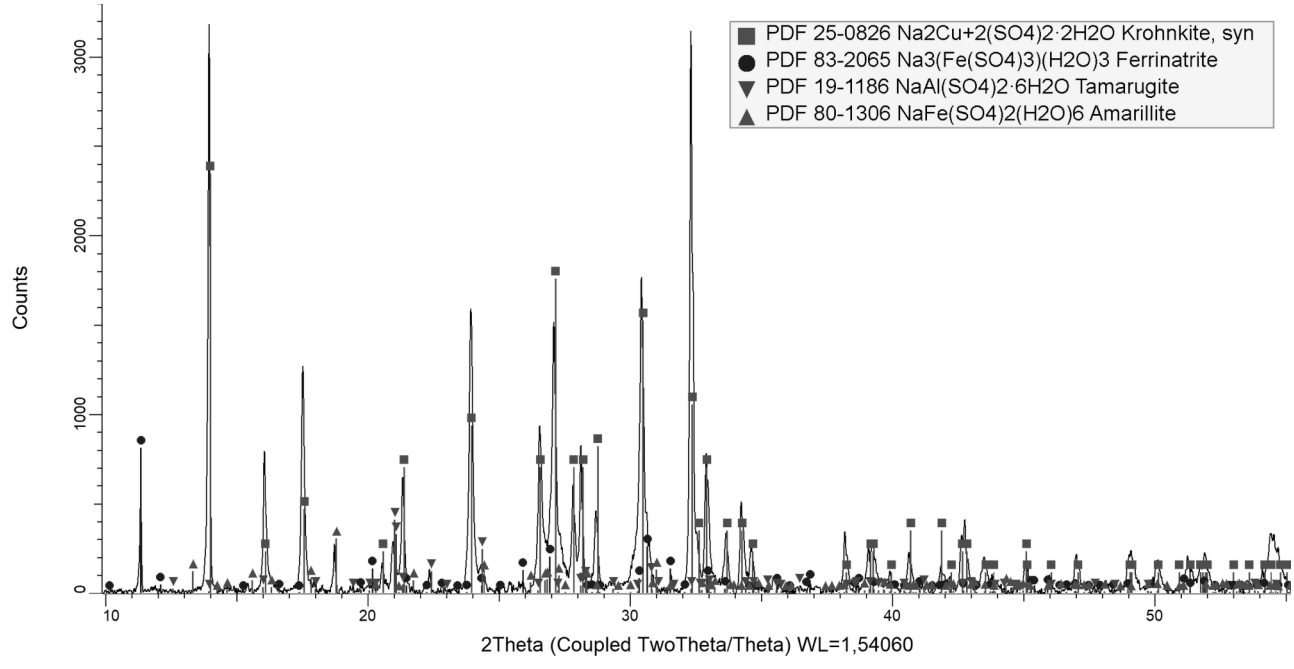

Figure 14. X-ray powder diffraction pattern of a ferrinatrite-, kröhnkite-, tamarugite-containing sample from Farbište ore deposit, Poniky, Slovakia

14. ábra. *Póniki (Farbište érctelep, Szlovákia) ferrinátrit-, kröhnkit- és tamarugittartalmú minta röntgenpordiffrakciós felvétele*

MÁNYI (1905). Closely associated with scorodite, bariopharmacosiderite forms rare 30–80 μm sized, green hexahedra, which were found during the reinvestigation of museum specimens collected in the early 20th century. The relative proportion of Ba and K varies in distinct zones of the individual hexahedra. The core is K-rich bariopharmacosiderite (dark grey in the BSE images), from core to rim it is bariopharmacosiderite (light grey in the BSE images) (*Figure 15*). The extensive cracking of the crystals is the result of subsequent oxidation. SEM-EDX measurements revealed that chemically inhomogeneous alteration products (Fe-As-containing Sb-oxides) are found on the surface and in the cracks of the crystals (*Figure 16*). The minerals of these earthy encrustations could not be identified more precisely due to their small amount and inhomogeneity. The above-described bariopharmacosiderite is an oxidation product of tetrahedrite.

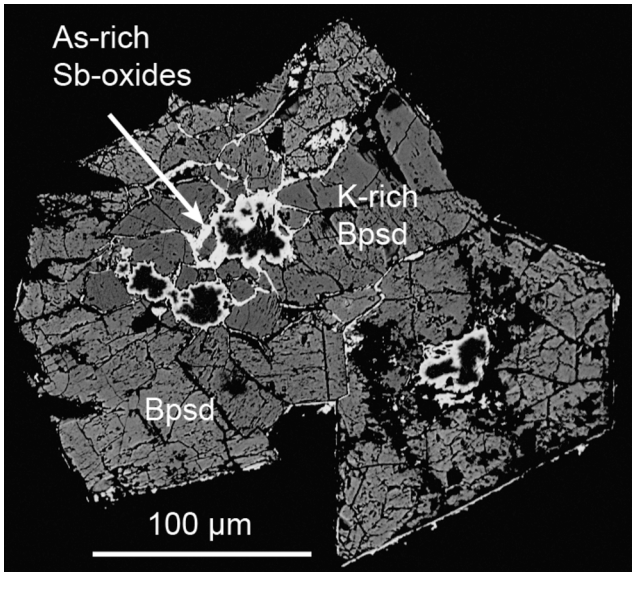

Figure 15. Bariopharmacosiderite (Bpsd, light grey) and K-rich bariopharmacosiderite (dark grey) with Sb oxide crusts (white) from Rožňava, Slovakia. BSE image. Photo by V. KOLLÁROVÁ

15. ábra. *Bariofarmakosziderit (Bpsd, világosszürke) és K-gazdag bariofarmakosziderit (sötétszürke) Sb-oxid kérgekkel (fehér). Rozsnyó (Szlovákia). Visszaszórtelektron-kép. Fotó: V. KOLLÁROVÁ*

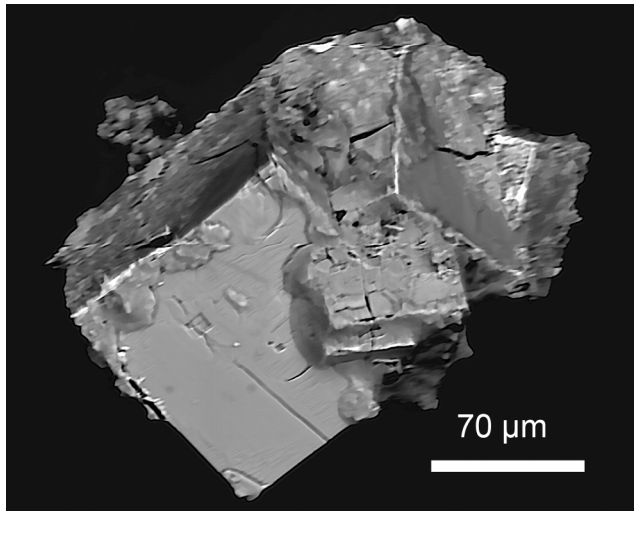

Figure 16. Chemically inhomogeneous Sb oxides on the surface of bariopharmacosiderite cubes. BSE image

16. ábra. *Kémiailag inhomogén Sb-oxid bekérgezés bariofarmakosziderit kockákon. Visszaszórtelektron-kép*

Acknowledgements

We thank Gábor KOLLER (Pilisborosjenő) for providing the kyrgyzstanite sample, and Rudolf ĎUĎA (Košice) for providing the kröhnkite and ferrinatrite samples. We also appreciate the help of Melinda JÁNOSI (Hungarian Natural History Museum, Budapest), and Bálint PÉTERDI (Supervisory Authority of Regulatory Affairs, Budapest) with selecting suitable samples for the investigations. Judith MIHÁLY (Institute of Materials and Environmental Chemistry, Eötvös Loránd Research Network, Budapest) is thanked for performing the FTIR measurements. We also thank the two referees, Gábor PAPP (Hungarian Natural History Museum, Budapest) and Mihály PÓSFAI (University of Pannonia, Veszprém) for improvements and comments on the manuscript.

The research was conducted at the University of Miskolc as part of the project supported by the Ministry of Innovation and Technology from the National Research, Development and Innovation Fund, according to the grant contract issued by the National Research, Development and Innovation Office (grant contract reg. nr.: TKP-17-1/PALY-2020).

References

AGAKHANOV, A. A., KARPENKO, V. YU. & PAUTOV, L. A. 2005: Kyrgyzstanite, $ZnAl_4(SO_4)(OH)_{12} \bullet 3H_2O$, a new mineral from the Kara-Tangi deposit, Kirgizia. – *New Data on Minerals* **40**, 23–28.

BAYLISS, P., KOLITSCH, U., NICKEL, E. H. & PRING, A. 2010: Alunite supergroup: recommended nomenclature. – *Mineralogical Magazine* **74**, 919–927. https://doi.org/10.1180/minmag.2010.074.5.919

DILL, H. G. 2001: The geology of aluminium phosphates and sulphates of the alunite group minerals: a review. – *Earth-Science Reviews* **53**, 35–93. https://doi.org/10.1016/S0012-8252(00)00035-0

FEHÉR, B. 2017: Foitite-magnesiofoitite from the Rózsa Hill ore mineralization, or re-investigation of the tourmaline from Nagybörzsöny, Börzsöny Mts., Hungary. – *Földtani Közlöny* **147**, 138–148 (in Hungarian). https://doi.org/10.23928/foldt.kozl.2017.147.2.133

FEHÉR, B., SZAKÁLL, S., KRISTÁLY, F. & ZAJZON, N. 2016: Mineralogical mosaics from the Carpathian-Pannonian region 3. – *Földtani Közlöny* **146**, 47–60.

HENRY, D. J., NOVÁK, M., HAWTHORNE, F. C., ERTL, A., DUTROW, B. L., UHER, P. & PEZZOTTA, F. 2011: Nomenclature of the tourmaline-supergroup minerals. – *American Mineralogist* **96**, 895–913. https://doi.org/10.2138/am.2011.3636

KODĚRA, M. (Ed.) 1986: *Topografická mineralogia Slovenska. Vol. 1.* – Veda Vydavatelstvo Slovenskej Akadémie Vied, Bratislava, 577 p. (in Slovak)

MANDARINO, J. A. & WILL, N. V. 1983: Weddellite from Biggs, Oregon, USA. – *Canadian Mineralogist* **21**, 503–508.

MOLNÁR, F., JUNG, P., KUPI, L., POGÁNY, A., VÁGÓ, E., VIKTORIK, O. & PÉCSKAY, Z. 2008: Epithermal zones of the porphyry-skarn-epithermal ore complex at Recsk. – In: FÖLDESSY, J., HARTAI, É. (eds): Recsk and Lahóca – Geology of the Paleogene ore complex. – *Publications of the University of Miskolc, Series A, Mining* **73**, 99–128.

PAPP, G. 1990: Szulfát ásványtársulás Tokodról. – *Földtani Közlöny* **120**, 83–89 (in Hungarian).

SCOTT, K. M. 1987: Solid solution in, and classification of, gossan-derived members of the alunite-jarosite family, northwest Queensland, Australia. – *American Mineralogist* **72**, 178–187.

STANCIU, C. 1976: Transformări hidrotermale în craterul Ostoroş (foraj 3) din Munţii Harghita. – *Dări de seamă ale şedinţelor* **62/1**, 199–213 (in Romanian).

SZAKÁLL S., FÖLDVÁRI M. & KOVÁCS Á. 1994: Foszfátásványok a recski és a parád-parádfürdői ércesedésekből. – *Folia Historico-Naturalia Musei Matraensis* **19**, 23–36 (in Hungarian).

SZAKÁLL, S. & KRISTÁLY, F. (eds) 2010: *Mineralogy of Székelyland, Eastern Transylvania, Romania*. – Csík County Nature and Conservation Society. Sf. Gheorghe, Miercurea Ciuc, Târgu Mureş, 321p.

WARR, L. N. 2021: IMA–CNMNC approved mineral symbols. – *Mineralogical Magazine* **85**, 291–320. doi:10.1180/mgm.2021.43

WEISZBURG, T. G., VINCZE, P., SZÖŐR, GY., LOVAS, GY. A. & BALLA, M. 2000: Mellite ($Al_2C_{12}O_{12} \bullet 16H_2O$) from Csordakút mine, Bicske, Hungary: a new mineral for the Carpathian-Pannonian region. – *Acta Mineralogica-Petrographica* **41**/Supplementum, 125.

ZIMÁNYI, K. 1905: Beiträge zur Mineralogie der Komitate Gömör und Abauj-Torna. – *Földtani Közlöny* **35**, 544–548.

Manuscript received: 22/11/2022

Appendix I

Electron-microprobe data of APS minerals from Lahóca Hill, Recsk (in wt.%)
APS-ásványok elektronmikroszondás elemzési adatai tömegszázalékban (Recsk, Lahóca)

SO_3	8.15	5.72	7.39	6.39	12.75	12.98	12.27	11.72	14.04	14.28
P_2O_5	26.50	28.32	27.15	26.58	19.51	20.18	20.46	21.20	16.93	14.09
As_2O_5	0.06	0.08	0.07	0.06	0.05	0.07	0.06	0.10	0.11	0.11
SiO_2	0.09	0.00	0.01	0.02	0.20	0.03	0.26	0.00	0.01	0.00
Al_2O_3	34.91	34.49	34.55	34.69	33.21	33.08	32.74	34.21	31.40	30.02
La_2O_3	0.00	0.04	0.01	0.00	0.03	0.04	0.01	0.00	0.00	0.03
Ce_2O_3	0.05	0.09	0.01	0.02	0.06	0.07	0.04	0.07	0.02	0.12
Yb_2O_3	0.03	0.01	0.02	0.07	0.05	0.03	0.00	0.03	0.16	0.04
MgO	0.00	0.00	0.00	0.00	0.00	0.00	0.00	0.00	0.00	0.00
CaO	12.54	11.08	12.54	11.51	5.83	6.30	7.06	8.18	7.07	3.79
MnO	0.00	0.00	0.00	0.00	0.00	0.00	0.02	0.03	0.02	0.00
FeO*	0.01	0.00	0.04	0.03	0.06	0.00	0.10	0.03	0.18	0.03
SrO	0.07	0.13	0.29	0.16	12.56	11.69	9.11	7.30	0.57	0.50
BaO	0.05	1.20	0.12	0.41	0.73	0.85	0.80	0.75	0.58	0.57
PbO	1.18	3.68	0.31	3.02	0.19	0.10	0.55	0.31	17.01	26.49
Na_2O	0.01	0.01	0.02	0.00	0.01	0.00	0.01	0.00	0.02	0.00
F	0.99	2.48	0.59	0.88	0.04	0.08	0.15	0.14	0.15	0.00
Cl			0.00	0.00	0.01	0.00	0.00	0.00	0.01	0.03
H_2O**	13.00	12.30	13.20	13.10	12.60	12.50	12.30	12.70	11.55	10.80
O = F, Cl	-0.41	-1.04	-0.25	-0.37	-0.02	-0.03	-0.06	-0.06	-0.06	-0.01
Total	**97.24**	**98.58**	**96.07**	**96.56**	**97.86**	**97.94**	**95.88**	**96.70**	**99.76**	**100.89**
Ion numbers based on 14 (O, OH, F, Cl) anions / Ionszámok 14 (O, OH, F, Cl) anionra										
S	0.44	0.31	0.40	0.35	0.72	0.73	0.70	0.66	0.84	0.92
P	1.61	1.75	1.66	1.65	1.25	1.28	1.32	1.34	1.15	1.02
As	0.00	0.00	0.00	0.00	0.00	0.00	0.00	0.00	0.00	0.01
Si	0.01	0.00	0.00	0.00	0.01	0.00	0.02	0.00	0.00	0.00
Σ*C*	**2.06**	**2.06**	**2.06**	**2.01**	**1.99**	**2.02**	**2.04**	**2.00**	**2.00**	**1.95**
Al	2.95	2.96	2.94	3.00	2.96	2.93	2.93	3.00	2.96	3.04
La	0.00	0.00	0.00	0.00	0.00	0.00	0.00	0.00	0.00	0.00
Ce	0.00	0.00	0.00	0.00	0.00	0.00	0.00	0.00	0.00	0.00
Yb	0.00	0.00	0.00	0.00	0.00	0.00	0.00	0.00	0.00	0.00
Σ*B*	**2.95**	**2.96**	**2.94**	**3.00**	**2.96**	**2.93**	**2.94**	**3.01**	**2.97**	**3.04**
Mg	0.00	0.00	0.00	0.00	0.00	0.00	0.00	0.00	0.00	0.00
Ca	0.96	0.86	0.97	0.91	0.47	0.51	0.58	0.65	0.61	0.35
Mn	0.00	0.00	0.00	0.00	0.00	0.00	0.00	0.00	0.00	0.00
Fe	0.00	0.00	0.00	0.00	0.00	0.00	0.01	0.00	0.01	0.00
Sr	0.00	0.01	0.01	0.01	0.55	0.51	0.40	0.32	0.03	0.02
Ba	0.00	0.03	0.00	0.01	0.02	0.02	0.02	0.02	0.02	0.02
Pb	0.02	0.07	0.01	0.06	0.00	0.00	0.01	0.01	0.37	0.61
Na	0.00	0.00	0.00	0.00	0.00	0.00	0.00	0.00	0.00	0.00
Σ*A*	**0.99**	**0.98**	**1.00**	**0.99**	**1.05**	**1.04**	**1.02**	**1.00**	**1.03**	**1.01**
OH	6.22	5.97	6.35	6.42	6.35	6.26	6.24	6.31	6.17	6.18
F	0.22	0.57	0.13	0.20	0.01	0.02	0.04	0.03	0.04	0.00
Cl	0.00	0.00	0.00	0.00	0.00	0.00	0.00	0.00	0.00	0.00
O	7.56	7.46	7.51	7.38	7.64	7.72	7.73	7.66	7.79	7.81
Σ anion	**14.00**	**14.00**	**14.00**	**14.00**	**14.00**	**14.00**	**14.00**	**14.00**	**14.00**	**14.00**
mineral* **	**Cdl**	**Cdl**	**Cdl**	**Cdl**	**Svb**	**Svb/Wdh**	**Wdh**	**Wdh**	**Wdh**	**Hda**

Appendix I – continued

SO_3	14.12	13.13	13.43	10.30	11.07	11.47	4.56	5.88	6.14	9.47
P_2O_5	16.13	16.86	12.90	21.69	21.21	21.48	26.67	25.34	25.58	23.61
As_2O_5	0.07	0.05	0.10	0.07	0.07	0.09	0.06	0.07	0.04	0.04
SiO_2	0.06	0.03	0.19	0.05	0.17	0.30	0.00	0.04	0.05	0.03
Al_2O_3	31.74	34.88	28.76	33.03	33.70	33.06	32.77	31.80	32.32	34.89
La_2O_3	0.00	0.00	0.00	0.00	0.03	0.00	0.01	0.00	0.00	0.05
Ce_2O_3	0.08	0.03	0.02	0.09	0.09	0.08	0.14	0.07	0.12	0.07
Yb_2O_3	0.07	0.07	0.04	0.00	0.09	0.02	0.03	0.04	0.04	0.03
MgO	0.00	0.00	0.00	0.00	0.00	0.00	0.00	0.00	0.00	0.00
CaO	6.57	8.97	3.12	6.23	7.09	7.18	3.60	4.01	4.14	11.74
MnO	0.00	0.00	0.01	0.00	0.04	0.01	0.01	0.00	0.01	0.02
FeO*	0.06	0.01	0.01	0.07	0.17	0.28	0.03	0.00	0.00	0.03
SrO	0.70	0.33	0.24	11.99	10.16	10.37	15.17	15.23	15.59	0.47
BaO	0.58	0.41	0.50	0.80	0.68	0.84	1.55	1.00	1.10	0.24
PbO	18.16	12.58	27.82	0.07	0.07	0.12	0.03	0.05	0.04	2.01
Na_2O	0.01	0.00	0.00	0.02	0.00	0.00	0.00	0.01	0.00	0.00
F	0.01	0.00	0.00	0.68	0.26	0.29	1.57	1.47	1.38	0.89
Cl	0.01	0.01	0.02	0.00	0.01	0.01	0.01	0.00	0.00	0.00
H_2O**	11.60	12.90	10.40	12.60	12.90	12.70	12.40	12.10	12.45	12.90
O = F, Cl	0.00	0.00	0.00	−0.29	−0.11	−0.12	−0.66	−0.62	−0.58	−0.37
Total	**99.96**	**100.26**	**97.55**	**97.42**	**97.71**	**98.19**	**97.95**	**96.49**	**98.44**	**96.10**
Ion numbers based on 14 (O, OH, F, Cl) anions / Ionszámok 14 (O, OH, F, Cl) anionra										
S	0.85	0.75	0.91	0.59	0.62	0.64	0.26	0.34	0.35	0.52
P	1.10	1.09	0.99	1.39	1.34	1.36	1.74	1.67	1.66	1.46
As	0.00	0.00	0.00	0.00	0.00	0.00	0.00	0.00	0.00	0.00
Si	0.00	0.00	0.02	0.00	0.01	0.02	0.00	0.00	0.00	0.00
Σ*C*	**1.96**	**1.85**	**1.92**	**1.98**	**1.98**	**2.03**	**2.00**	**2.02**	**2.02**	**1.99**
Al	3.02	3.14	3.07	2.95	2.97	2.91	2.97	2.92	2.91	3.01
La	0.00	0.00	0.00	0.00	0.00	0.00	0.00	0.00	0.00	0.00
Ce	0.00	0.00	0.00	0.00	0.00	0.00	0.00	0.00	0.00	0.00
Yb	0.00	0.00	0.00	0.00	0.00	0.00	0.00	0.00	0.00	0.00
Σ*B*	**3.02**	**3.14**	**3.07**	**2.95**	**2.97**	**2.91**	**2.98**	**2.93**	**2.92**	**3.02**
Mg	0.00	0.00	0.00	0.00	0.00	0.00	0.00	0.00	0.00	0.00
Ca	0.57	0.73	0.30	0.51	0.57	0.57	0.30	0.34	0.34	0.92
Mn	0.00	0.00	0.00	0.00	0.00	0.00	0.00	0.00	0.00	0.00
Fe	0.00	0.00	0.00	0.00	0.01	0.02	0.00	0.00	0.00	0.00
Sr	0.03	0.01	0.01	0.53	0.44	0.45	0.68	0.69	0.69	0.02
Ba	0.02	0.01	0.02	0.02	0.02	0.02	0.05	0.03	0.03	0.01
Pb	0.39	0.26	0.68	0.00	0.00	0.00	0.00	0.00	0.00	0.04
Na	0.00	0.00	0.00	0.00	0.00	0.00	0.00	0.00	0.00	0.00
Σ*A*	**1.02**	**1.02**	**1.01**	**1.07**	**1.04**	**1.07**	**1.02**	**1.06**	**1.07**	**0.99**
OH	6.24	6.57	6.27	6.36	6.43	6.32	6.36	6.29	6.35	6.30
F	0.00	0.00	0.00	0.16	0.06	0.07	0.38	0.36	0.33	0.21
Cl	0.00	0.00	0.00	0.00	0.00	0.00	0.00	0.00	0.00	0.00
O	7.76	7.43	7.72	7.47	7.51	7.61	7.25	7.34	7.31	7.49
Σ anion	**14.00**	**14.00**	**14.00**	**14.00**	**14.00**	**14.00**	**14.00**	**14.00**	**14.00**	**14.00**
mineral* **	**Wdh**	**Wdh**	**Hda**	**Svb**	**Wdh**	**Wdh**	**Goy**	**Goy**	**Goy**	**Wdh**

* Total iron was measured as FeO / Az összes vas FeO-ként mérve

** H_2O was calculated from the stoichiometry: A + B + C = 6 *apfu* / H_2O a sztöchiometrikus összetételből számolva: A + B + C = 6 *apfu*

*** Minerals / ásványok (Warr 2021): Cdl = crandallite/crandallit, Goy = goyazite/goyazit, Hda = hinsdalite/hinsdalit, Svb = svanbergite/svanbergit, Wdh = woodhouseite/woodhouseit

Appendix II

Electron-microprobe data of tourmaline from Harghita Mts. (in wt.%)
Hargitai turmalinok elektronmikroszondás elemzési adatai tömegszázalékban

	1	2	3	4	5	6	7	8	9	10	11	12
SiO_2	34.27	35.20	35.72	36.85	35.72	34.62	34.10	36.19	36.54	36.29	36.29	34.66
TiO_2	0.05	0.04	0.08	0.08	0.09	0.07	0.07	0.22	0.11	0.20	0.11	0.02
B_2O_3*	10.86	10.88	11.02	11.06	11.03	10.96	10.90	10.82	10.79	10.83	10.75	10.58
Al_2O_3	39.68	38.33	38.73	37.59	38.76	39.97	39.77	36.86	36.45	36.86	36.41	37.08
Cr_2O_3	0.00	0.02	0.04	0.00	0.00	0.01	0.01	0.00	0.00	0.02	0.00	0.00
FeO**	0.18	0.46	0.25	0.27	0.41	0.15	0.21	6.49	8.17	6.89	7.65	5.25
MgO	7.57	8.01	8.01	8.60	8.10	7.68	7.90	4.76	3.69	4.46	3.93	5.18
CaO	1.97	1.60	1.73	1.42	1.70	1.84	2.01	0.69	0.67	0.71	0.71	1.25
MnO	0.01	0.06	0.06	0.05	0.04	0.05	0.01	0.15	0.22	0.15	0.20	0.01
Na_2O	0.85	1.12	1.20	1.08	1.18	0.92	0.96	1.32	1.19	1.32	1.23	0.83
K_2O	0.01	0.02	0.02	0.02	0.01	0.02	0.01	0.03	0.02	0.02	0.02	0.01
F	0.12	0.11	0.10	0.07	0.08	0.10	0.10	0.69	0.62	0.78	0.68	0.01
Cl	0.07	0.04	0.04	0.02	0.02	0.03	0.06	0.03	0.02	0.02	0.04	0.34
H_2O***	3.67	3.69	3.74	3.78	3.76	3.73	3.70	3.40	3.42	3.36	3.38	3.56
O = F, Cl	−0.05	−0.05	−0.04	−0.03	−0.03	−0.04	−0.04	−0.29	−0.26	−0.33	−0.29	0.00
Total	**99.27**	**99.54**	**100.70**	**100.86**	**100.87**	**100.11**	**99.77**	**101.36**	**101.65**	**101.58**	**101.11**	**98.78**
Ion numbers based on 31 (O, OH, F, Cl) anions / Ionszámok 31 (O, OH, F, Cl) anionra												
Si	5.48	5.62	5.63	5.79	5.63	5.49	5.44	5.81	5.89	5.82	5.87	5.69
Al	0.52	0.38	0.37	0.21	0.37	0.51	0.56	0.19	0.11	0.18	0.13	0.31
Σ*T*	**6.00**	**6.00**	**6.00**	**6.00**	**6.00**	**6.00**	**6.00**	**6.00**	**6.00**	**6.00**	**6.00**	**6.00**
B	3.00	3.00	3.00	3.00	3.00	3.00	3.00	3.00	3.00	3.00	3.00	3.00
Σ*B*	**3.00**	**3.00**	**3.00**	**3.00**	**3.00**	**3.00**	**3.00**	**3.00**	**3.00**	**3.00**	**3.00**	**3.00**
Al	6.00	6.00	6.00	6.00	6.00	6.00	6.00	6.00	6.00	6.00	6.00	6.00
Cr	0.00	0.00	0.00	0.00	0.00	0.00	0.00	0.00	0.00	0.00	0.00	0.00
Σ*Z*	**6.00**	**6.00**	**6.00**	**6.00**	**6.00**	**6.00**	**6.00**	**6.00**	**6.00**	**6.00**	**6.00**	**6.00**
Al	0.96	0.83	0.84	0.75	0.82	0.96	0.91	0.79	0.81	0.80	0.81	0.87
Ti	0.01	0.00	0.01	0.01	0.01	0.01	0.01	0.03	0.01	0.02	0.01	0.00
Mg	1.81	1.91	1.88	2.01	1.90	1.82	1.88	1.14	0.89	1.07	0.95	1.27
Mn	0.00	0.01	0.01	0.01	0.01	0.01	0.00	0.02	0.03	0.02	0.03	0.00
Fe^{2+}	0.02	0.06	0.03	0.04	0.05	0.02	0.03	0.87	1.10	0.92	1.03	0.72
Σ*Y*	**2.80**	**2.82**	**2.77**	**2.82**	**2.80**	**2.81**	**2.83**	**2.85**	**2.84**	**2.83**	**2.83**	**2.86**
Ca	0.34	0.27	0.29	0.24	0.29	0.31	0.34	0.12	0.12	0.12	0.12	0.22
Na	0.26	0.35	0.37	0.33	0.36	0.28	0.30	0.41	0.37	0.41	0.39	0.26
K	0.00	0.00	0.00	0.00	0.00	0.00	0.00	0.01	0.00	0.00	0.00	0.00
[]	0.40	0.38	0.34	0.43	0.35	0.40	0.36	0.46	0.51	0.46	0.49	0.51
Σ*X*	**1.00**	**1.00**	**1.00**	**1.00**	**1.00**	**1.00**	**1.00**	**1.00**	**1.00**	**1.00**	**1.00**	**1.00**
OH	3.92	3.93	3.94	3.96	3.95	3.94	3.93	3.64	3.68	3.60	3.64	3.90
F	0.06	0.06	0.05	0.03	0.04	0.05	0.05	0.35	0.32	0.40	0.35	0.01
Cl	0.02	0.01	0.01	0.01	0.01	0.01	0.02	0.01	0.01	0.01	0.01	0.09
Σ (*V*+*W*)	**4.00**	**4.00**	**4.00**	**4.00**	**4.00**	**4.00**	**4.00**	**4.00**	**4.00**	**4.00**	**4.00**	**4.00**
mineral**	**Mfoi**	**Mfoi**	**Drv**	**Mfoi**	**Drv**	**Mfoi**	**Mfoi**	**Mfoi**	**Foi**	**Mfoi**	**Foi**	**Mfoi**

* B_2O_3 was calculated from the stoichiometry: B = 3 *apfu* / B_2O_3 a sztöchiometrikus összetételből számolva: B = 3 *apfu*
** Total iron was measured as FeO / Összes vas FeO-ként mérve
*** H_2O was calculated from the stoichiometry: OH + F + Cl = 4 *apfu* / H_2O a sztöchiometrikus összetételből számolva: OH + F + Cl = 4 *apfu*
**** Minerals / ásványok (Warr 2021): Drv = dravite/drávit, Foi = foitite/foitit, Mfoi = magnesio-foitite/magneziofoitit

Appendix III

X-ray powder diffraction data of kröhnkite from Poniky in comparison with those of the ICDD 00-070-0884 card
A póniki kröhnkit röntgen-pordiffrakciós adatai, összehasonlítva az ICDD 00-070-0884 kártya megfelelő adataival

Kröhnkite Poniky		Kröhnkite (ICDD 00-070-0884)					Kröhnkite Poniky		Kröhnkite (ICDD 00-070-0884)				
d (Å)	*I* (%)	*d* (Å)	*I* (%)	*h*	*k*	*l*	*d* (Å)	*I* (%)	*d* (Å)	*I* (%)	*h*	*k*	*l*
6.35	88	6.328	100	0	2	0	1.854	9	1.853	13	−1	5	2
5.51	33	5.513	24	1	0	0	1.833	6	1.838	1	3	0	0
5.05	48	5.054	37	1	1	0	1.820	11	1.820	11	−1	1	3
4.31	8	4.310	12	−1	1	1	1.781	10	1.779	14	1	6	1
4.16	33	4.157	46	1	2	0	1.775	6	1.774	8	−3	1	2
3.71	69	3.712	67	−1	2	1	1.766	7	1.766	7	−1	2	3
3.35	31	3.350	33	1	3	0	1.763	9	1.762	7	1	4	2
3.29	68	3.285	89	0	3	1	1.760	15	1.758	13	−3	3	1
3.20	23	3.205	37	1	1	1	1.693	9	1.692	6	−2	6	1
3.17	22	3.164	18	0	4	0	1.686	19	1.685	16	3	3	0
3.11	23	3.104	42	−1	3	1	1.680	11	1.681	12	−2	2	3
2.93	76	2.935	92	1	2	1	1.675	8	1.675	11	2	6	0
2.76	100	2.765	79	−2	1	1	1.669	6	1.667	5	−1	6	2
2.75	15	2.756	49	2	0	0	1.655	7	1.656	1	2	0	2
2.74	11	2.744	21	1	4	0	1.650	7	1.650	4	−3	4	1
2.72	34	2.720	41	−1	0	2	1.645	7	1.643	8	0	6	2
2.66	16	2.659	18	−1	1	2	1.613	9	1.613	11	0	3	3
2.61	23	2.619	21	0	0	2	1.589	7	1.589	6	−1	4	3
2.58	13	1.586	18	−2	2	1	1.573	6	1.573	3	3	1	1
2.56	7	2.564	3	0	1	2	1.560	6	1.560	10	−3	4	2
2.52	6	2.527	2	2	2	0	1.553	8	1.552	4	−2	6	2
2.35	13	2.352	9	−2	3	1	1.539	6	1.537	2	3	2	1
2.30	13	2.300	9	1	5	0	1.527	7	1.529	1	0	4	3
2.29	13	2.292	9	−2	0	2	1.525	7	1.524	4	−2	7	1
2.29	8	2.286	5	−1	3	2	1.520	6	1.520	6	1	8	0
2.26	8	2.255	8	−2	1	2	1.487	6	1.488	2	0	7	2
2.21	11	2.216	21	−1	5	1	1.468	11	1.467	13	2	4	2
2.15	8	2.155	8	−2	2	2	1.463	6	1.463	7	−3	5	2
2.14	6	2.142	3	2	1	1	1.436	6	1.437	4	0	5	3
2.11	18	2.121	12	1	0	2	1.419	6	1.420	1	−2	7	2
2.11	12	2.109	7	−2	4	1	1.378	8	1.378	4	1	4	3
2.07	8	2.078	11	2	4	0	1.375	8	1.375	9	1	7	2
2.07	6	2.063	5	−1	4	2	1.372	6	1.371	5	2	8	0
2.01	12	2.011	15	1	5	1	1.357	6	1.358	1	0	9	1
1.93	11	1.932	13	2	3	1	1.355	6	1.354	2	0	8	2
1.85	14	1.856	13	−2	4	2	1.353	6	1.352	1	−2	1	4